

## Supporting information

### Synthesis of Amino functionalized Ti-MOF derived Yolk-Shell and Hollow heterostructures for enhanced Photocatalytic Hydrogen Production under visible light.

*Rehana Bibi<sup>a</sup>, Hailu Huang<sup>a</sup>, Mulenga Kalulu<sup>a</sup>, Quanhao Shen<sup>a</sup>, Lingfei Wei<sup>a</sup>, Olayinka Oderinde<sup>a</sup>, Naixu Li <sup>a\*</sup>, Jiancheng Zhou<sup>a,b,c\*</sup>*

*<sup>a</sup>School of Chemistry and Chemical Engineering, Southeast University, Nanjing, 211189, P.R. China.*

*<sup>b</sup>Department of Chemical and Pharmaceutical Engineering, Southeast University, Chengxian College, Nanjing, 210088, P.R. China.*

*<sup>c</sup>Jiangsu Province Hi-Tech Key Laboratory for Biomedical Research, Southeast University, Nanjing 211189, PR China.*

*\*Corresponding Author.*

*Tel : (+86) 025-52090621; fax: (+86) 025-52090620.*

*E-mail: jczhou@seu.edu.cn (Dr. Jiancheng Zhou)*

*Tel: +86 025-52090621; fax: +86 025-52090620*

*E-mail: naixuli@seu.edu.cn (Dr. Naixu Li)*

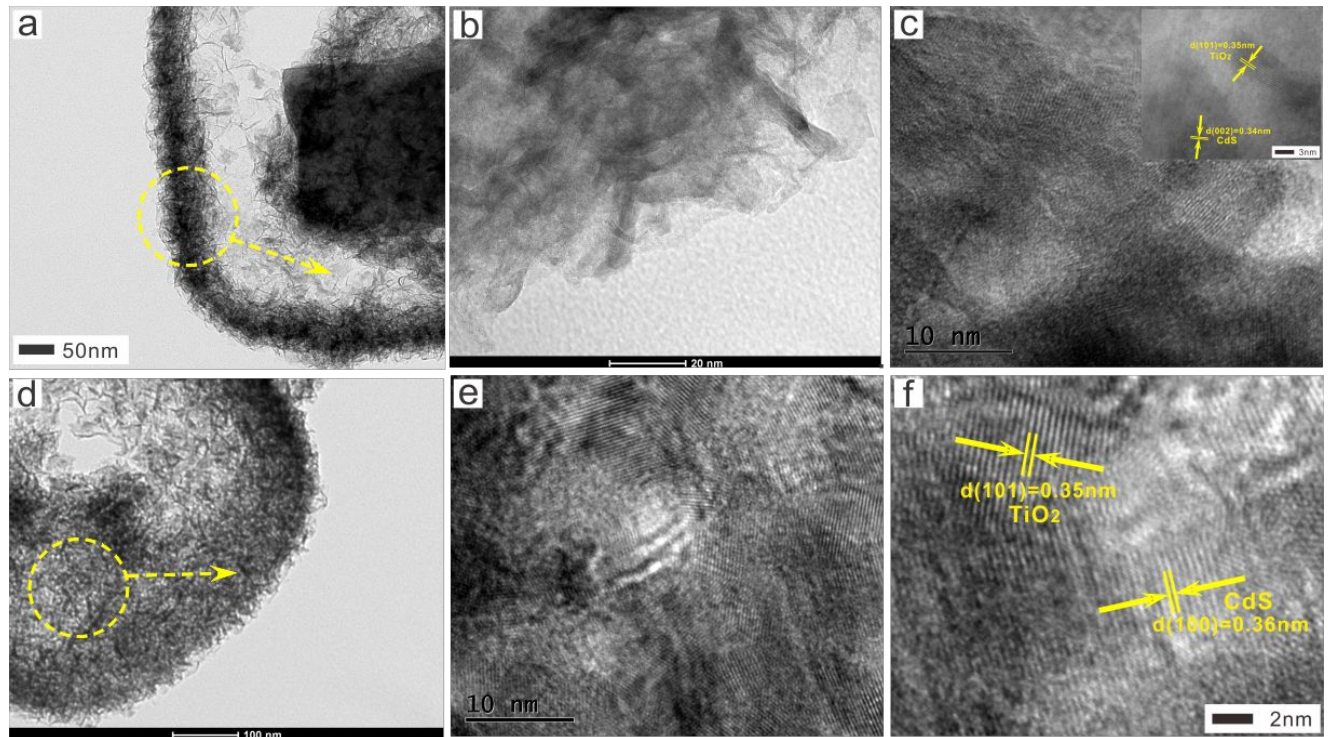


**Fig. S.1.** HRTEM image of (a-c)  $\text{NH}_2\text{-MIL-125/TiO}_2/\text{CdS}$  (30) (d-f)  $\text{H-TiO}_2/\text{CdS}$  (30).

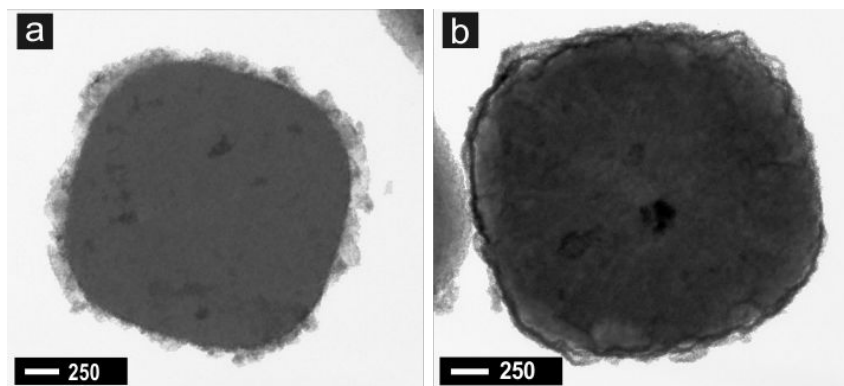


**Fig.S.2.** (a) MOF stability in ethanol at  $70^\circ\text{C}$  (2) MOF stability in methanol at  $70^\circ\text{C}$ .

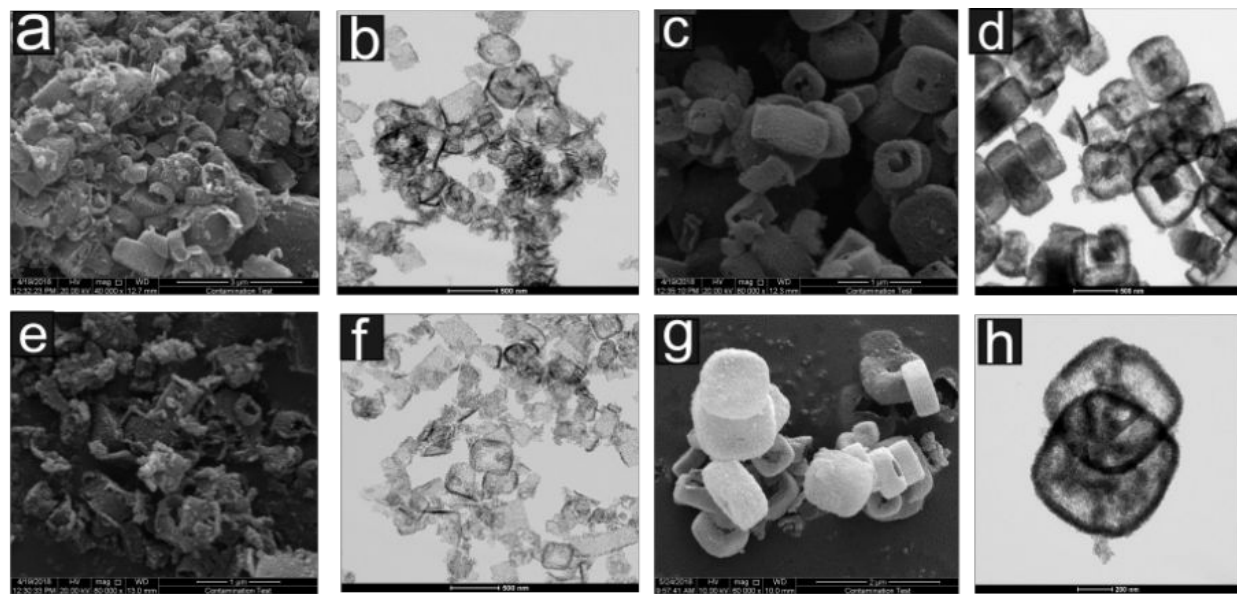


**Fig.S.3.** (a-b) SEM and TEM images of NH<sub>2</sub>-MIL-125-thioacetamide (TAA) for one-hour (c-d) NH<sub>2</sub>-MIL-125 + TAA+(Cd (CH<sub>3</sub>COO)<sub>2</sub>.2H<sub>2</sub>O) (e-f) NH<sub>2</sub>-MIL-125 + TAA for two-hours. (g-h) NH<sub>2</sub>-MIL-125 + TAA+(Cd (CH<sub>3</sub>COO)<sub>2</sub>.2H<sub>2</sub>O) for two-hours.

**Table S1.** CdS amount of heterostructures by ICP-MS analysis.

Samples	Wt % (ICP-MS)	
	Cd	S
NH <sub>2</sub> -MIL-125/TiO <sub>2</sub> /CdS (30)	18.575	3.601
H-TiO <sub>2</sub> /CdS (30)	27.257	5.933

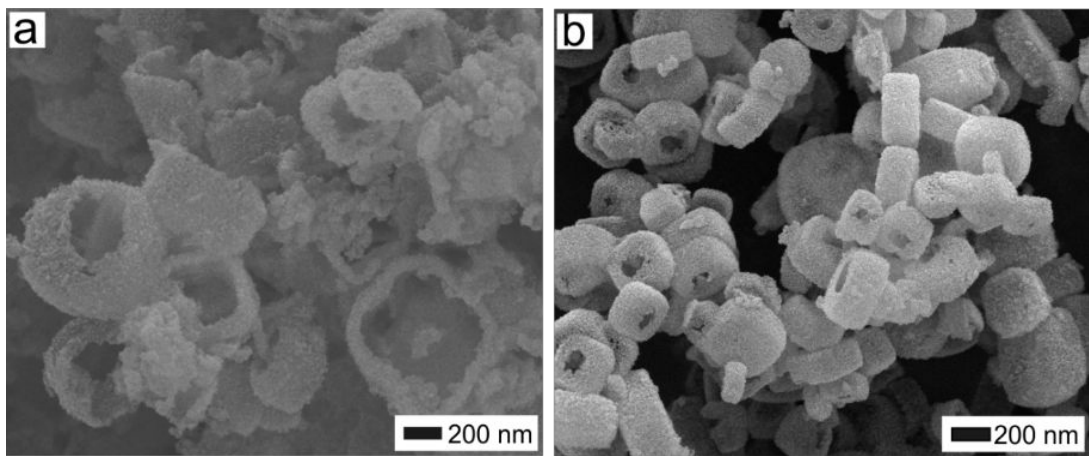


**Fig.S.4.** (a) SEM image of MOF + $\text{CdCl}_2\cdot 5\text{H}_2\text{O}$  + TAA (b) SEM image of MOF + $(\text{CH}_3\text{COO})_2\cdot 2\text{H}_2\text{O}$ ) + TAA.

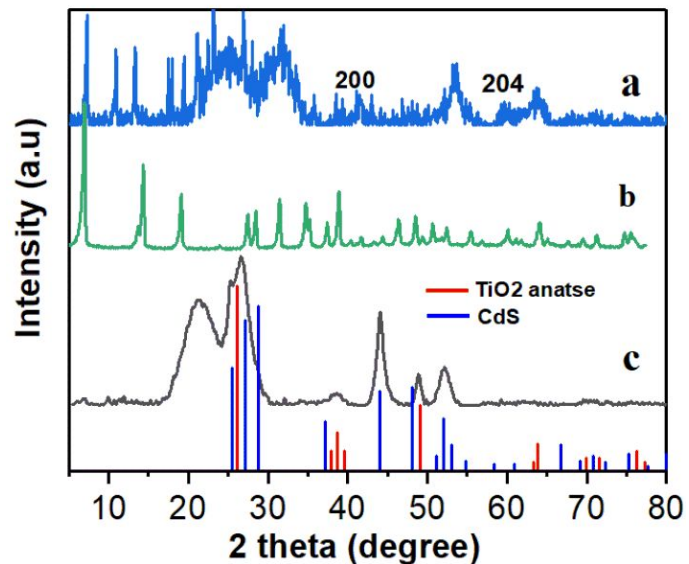


**Fig.S. 5.** XRD spectra of (a)  $\text{NH}_2\text{-MIL-125}/\text{TiO}_2/\text{CdS}$  (30) (b)  $\text{NH}_2\text{-MIL-125}$  (c)  $\text{H-TiO}_2/\text{CdS}$  (30).

### XPS spectral analysis of H-TiO<sub>2</sub>/CdS(30).

In the XPS spectrum of H-TiO<sub>2</sub>/CdS, the high-resolution Ti 2p spectrum shows two distinct peaks at 464.6 eV and 458.8 eV binding energy values, respectively, indicating that titanium binded with oxygen remained in the oxidation state of IV for the titanium oxo cluster<sup>1</sup>. The Cd 3d spectrum consists of two distinct peaks at 411.61 eV ( $3d_{3/2}$ ) and 404.86 eV ( $Cd\ 3d_{5/2}$ ) with a splitting energy of 6.7 eV, indicating the successful formation of CdS nanoparticles in the heterostructure.<sup>2</sup> Moreover the binding energies correspond to S $2p_{3/2}$  and S $2p_{1/2}$  are at 161.2eV and 162.36 eV indicating the presence of -2 S in CdS nanoparticles<sup>3</sup>.

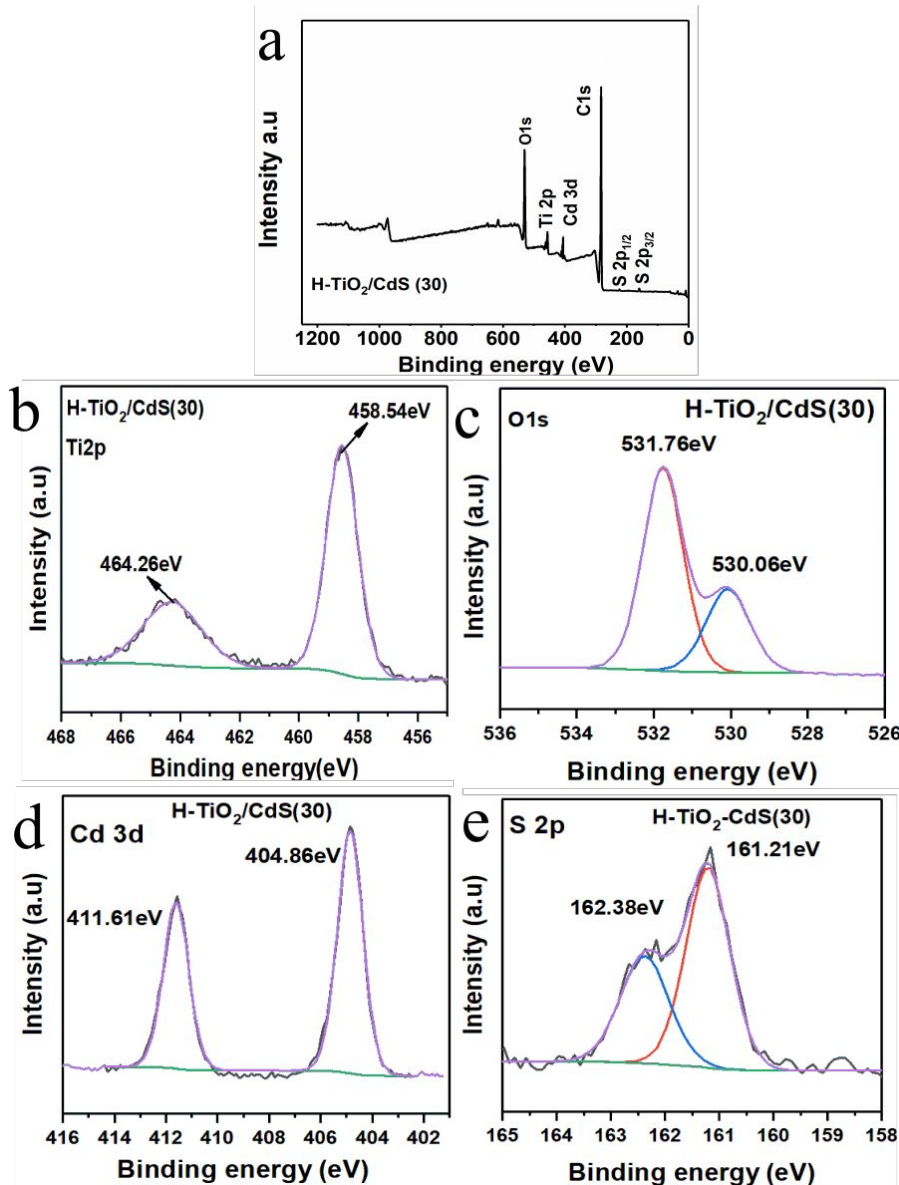


**Fig. S.6.** XPS spectra of H-TiO<sub>2</sub>/CdS (30).

**Electrochemical impedance spectroscopy.**

The photoinduced charge separation and transfer were further evaluated by electrochemical impedance spectroscopy (EIS). For comparison purposes, NH<sub>2</sub>-MIL-125 derived heterostructures (NH<sub>2</sub>-MIL-125/TiO<sub>2</sub> and hollow TiO<sub>2</sub> without CdS nanoparticles were prepared by the Bingxing Zhang method <sup>4</sup>, followed by measuring their EIS spectra. The experimental results shown in Figure S.7, revealed that with the addition of CdS nanoparticles, the photocatalytic activity MOF derived heterostructures increases.

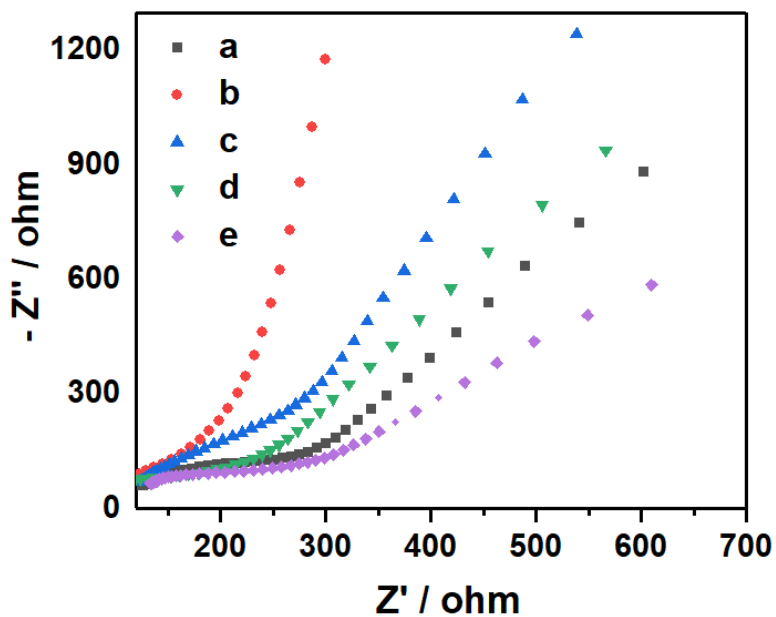


**Fig. S.7.** Nyquist plots of (a)H-TiO<sub>2</sub>/CdS (30) (b) MOF derived hollow TiO<sub>2</sub> (no CdS) (c) NH<sub>2</sub>-MIL-125 (d) NH<sub>2</sub>-MIL-125@TiO<sub>2</sub> (e) NH<sub>2</sub>-MIL-125/TiO<sub>2</sub>/CdS (30).

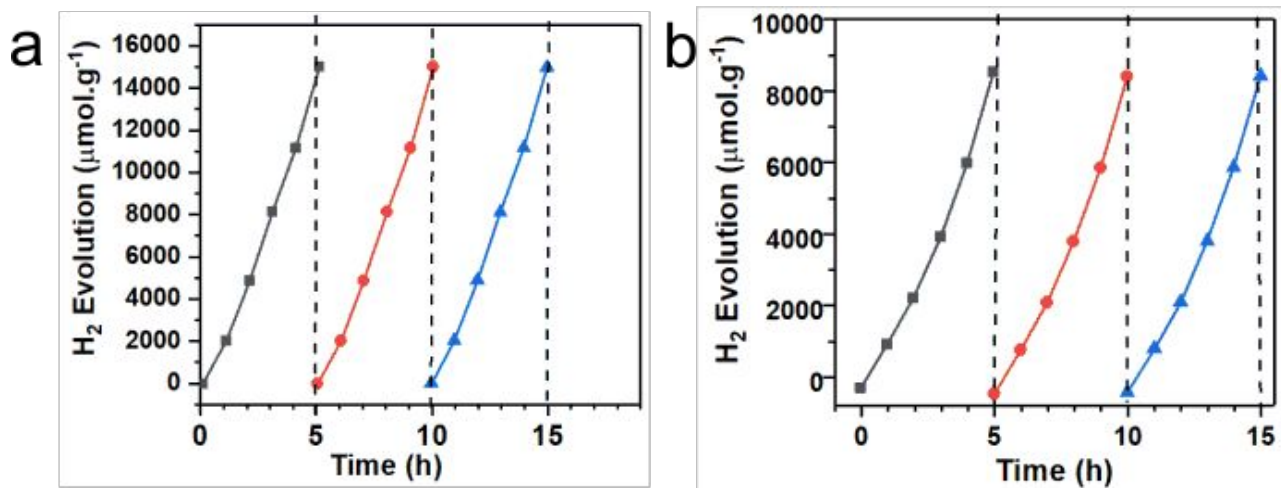


**Fig. S.8.** recycling test for H<sub>2</sub> production of (a) NH<sub>2</sub>-MIL-125/TiO<sub>2</sub>/CdS (30), (b) H-TiO<sub>2</sub>/CdS(30)

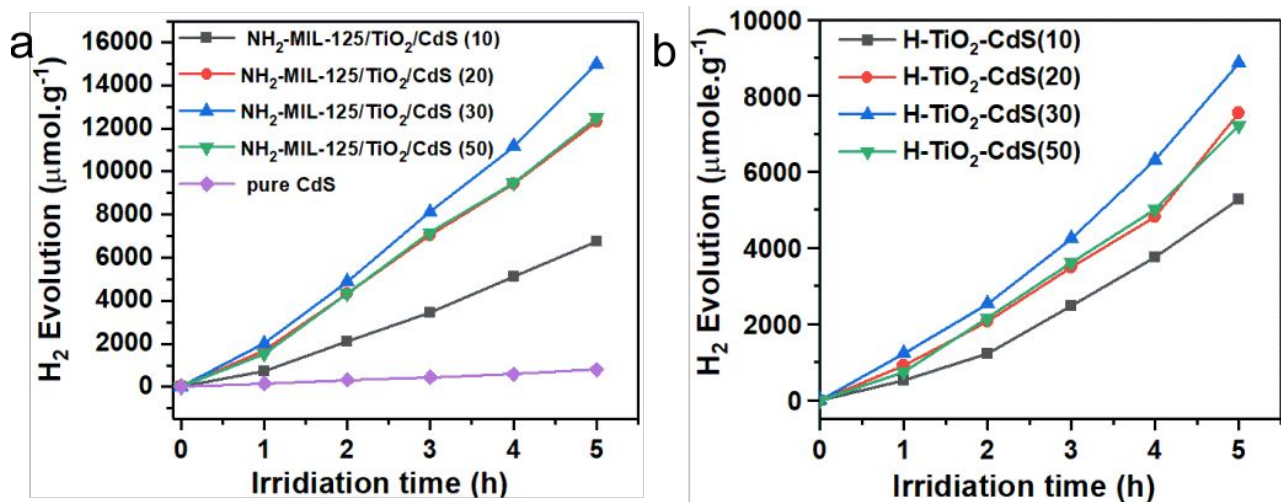


**Fig. S.9.** Photocatalytic H<sub>2</sub> evolution of various yolk-shell and hollow heterostructures with respect to time (a) NH<sub>2</sub>-MIL-125/TiO<sub>2</sub>/CdS (x) (b) H-TiO<sub>2</sub>/CdS(x).

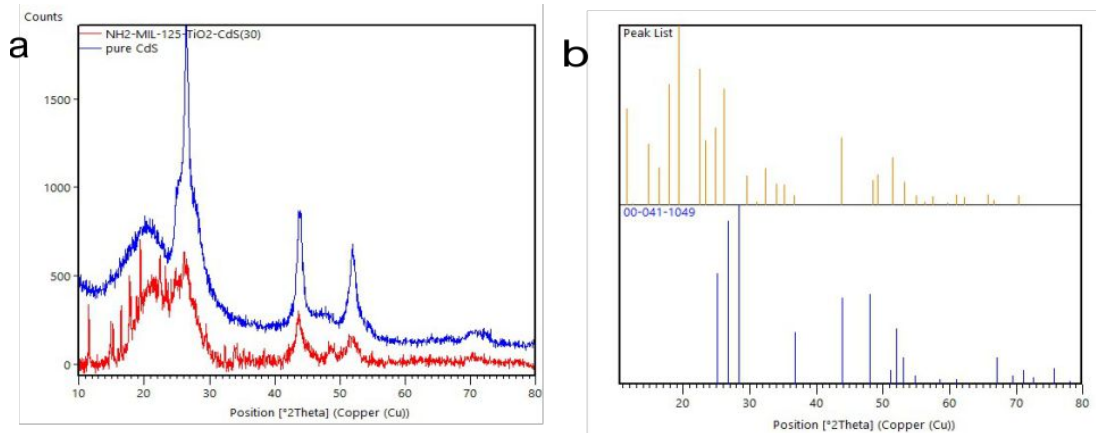


**Fig.S.10 (a-b)** XRD patterns of NH<sub>2</sub>-MIL-125/TiO<sub>2</sub>/CdS(30) with reference.

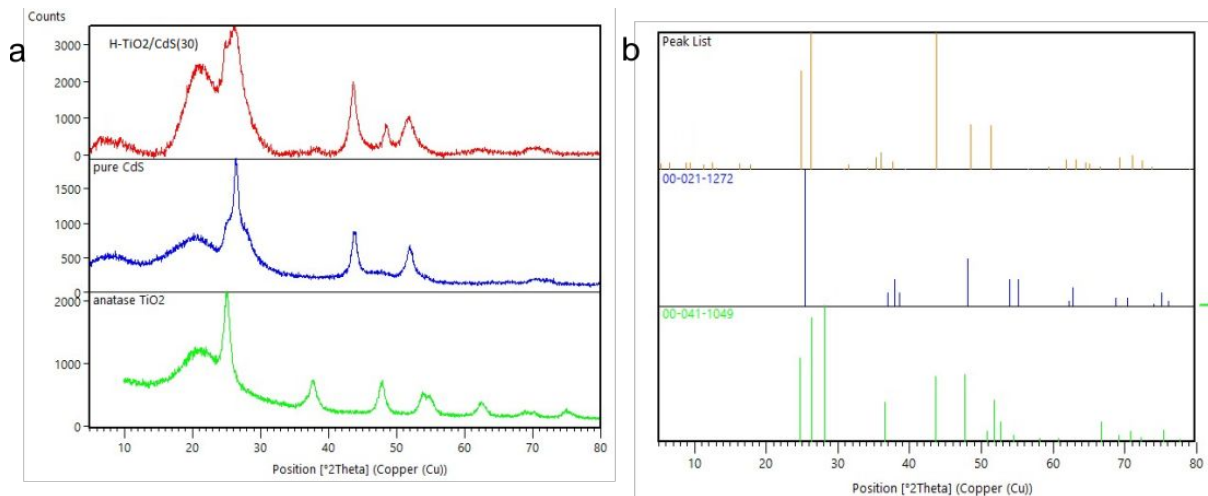


**Fig.S.11.(a-b)** XRD patterns of H-TiO<sub>2</sub>/CdS(30) with reference.

## References

1. Biesinger, M. C.; Lau, L. W. M.; Gerson, A. R.; Smart, R. S. C., Resolving surface chemical states in XPS analysis of first row transition metals, oxides and hydroxides: Sc, Ti, V, Cu and Zn. *Applied Surface Science* **2010**, *257* (3), 887-898 DOI: 10.1016/j.apsusc.2010.07.086.
2. Gao, C.; Zhang, Z.; Li, X.; Chen, L.; Wang, Y.; He, Y.; Teng, F.; Zhou, J.; Han, W.; Xie, E., Synergistic effects in three-dimensional SnO<sub>2</sub>/TiO<sub>2</sub>/CdS multi-heterojunction structure for highly efficient

photoelectrochemical hydrogen production. *Solar Energy Materials and Solar Cells* **2015**, *141*, 101-107  
DOI: 10.1016/j.solmat.2015.05.026.

3. Zhang, J.; Zhu, W.; Liu, X., Stable hydrogen generation from vermiculite sensitized by CdS quantum dot photocatalytic splitting of water under visible-light irradiation. *Dalton Trans* **2014**, *43* (24), 9296-302 DOI: 10.1039/c4dt00897a.

4. Zhang, B.; Zhang, J.; Tan, X.; Shao, D.; Shi, J.; Zheng, L.; Zhang, J.; Yang, G.; Han, B., MIL-125-NH<sub>2</sub>@TiO<sub>2</sub> Core-Shell Particles Produced by a Post-Solvothermal Route for High-Performance Photocatalytic H<sub>2</sub> Production. *ACS Appl Mater Interfaces* **2018**, *10* (19), 16418-16423 DOI: 10.1021/acsami.8b01462.